

Preparation of Sn doped nanometric TiO₂ powders by reflux and hydrothermal syntheses and their characterization

Nadir Kiraz · Esin Burunkaya · Ömer Kesmez ·
Hasan Erdem Çamurlu · Meltem Asiltürk ·
Zerin Yeşil · Ertuğrul Arpaç

Received: 15 January 2011 / Accepted: 6 June 2011 / Published online: 7 July 2011
© Springer Science+Business Media, LLC 2011

Abstract Hydrothermal and reflux synthesis methods were utilized for the preparation of 5% Sn doped TiO₂ nanopowders. Obtained powders were subjected to particle size and specific surface area measurements, flame atomic absorption spectroscopy, X-ray diffraction analyses and transmission electron microscopy examination. TiO₂ powder prepared by hydrothermal synthesis presented a bimodal particle size distribution with average particle sizes of about 3 and 10 nm, whereas TiO₂ powder synthesized by reflux method had an average particle size of 7 nm. Specific surface areas of hydrothermal and reflux synthesized TiO₂ were 130 and 115 m²/g, respectively. Sn doping in TiO₂ was 95.8% in hydrothermal and 86.4% in reflux synthesis as measured by FAAS, respectively. Photocatalytic activities of the obtained TiO₂ powders were evaluated by decomposition of malachite green solution in a solar box. Photocatalytic activity of hydrothermally

synthesized TiO₂ was fairly higher in visible light and slightly higher in UV light than the activity of reflux synthesized TiO₂.

Keywords Nano particle · TiO₂ · Photocatalysis · Hydrothermal synthesis · Reflux synthesis

1 Introduction

TiO₂ powder in nanometric form has been widely utilized as a pigment, as an additive in paints and in ointments, and in photovoltaic and electrochromic applications. It has also been used in photocatalytic sterilization, self-cleaning (SC), organic contaminant treatment and air purification applications due to its well-known photocatalytic effect [1–5]. Photocatalysis is essentially the breakdown of organic pollutant compounds on the surface of TiO₂, with the aid of ultraviolet (UV) or visible (VIS) light [1–3, 6]. The SC property of TiO₂ in both powder and film form has been widely investigated [1, 2, 4, 5, 7, 8], however, these studies mostly dealt with TiO₂ powder [2, 7, 8]. The efficiency of photocatalysts in powder form is superior to films due to the much larger specific surface area of powders, which provides relatively shorter duration of photocatalytic cleaning reactions.

Removal of organic contaminants in wastewater is an important issue for preventing the pollution of environment and preserving the clean water sources. Dyes, arising especially from textile industry are toxic pollutants that are present in industrial wastewater. Their treatment via physical or biological means is difficult. Utilization of TiO₂ as a promising heterogeneous photocatalyst for removal of organic pollutants from industrial wastewater has emerged in the last decade.

N. Kiraz (✉) · E. Burunkaya · Ö. Kesmez · Z. Yeşil · E. Arpaç
Department of Chemistry, Akdeniz University, Dumlupınar
Bulvarı, Kampüs, 07102 Antalya, Turkey
e-mail: nadirkiraz@akdeniz.edu.tr

N. Kiraz · E. Burunkaya · Ö. Kesmez · Z. Yeşil · E. Arpaç
NANOen R&D Ltd., Antalya Technopolis, Akdeniz University
Campus, 07102 Antalya, Turkey

H. E. Çamurlu
Department of Mechanical Engineering, Akdeniz University,
Dumlupınar Bulvarı, Kampüs, 07058 Antalya, Turkey

H. E. Çamurlu
Mattek R&D Ltd., Antalya Technopolis, Akdeniz University
Campus, 07058 Antalya, Turkey

M. Asiltürk
Department of Chemistry, İnönü University, 44280 Malatya,
Turkey

Many oxides have suitable band gap for photocatalysis. Among them, TiO_2 has attracted attention since it encompasses better properties such as low cost, non-toxicity and chemical stability. One significant downside of TiO_2 for SC applications is its wide band gap ($E_g = 3.2$ eV), which bounds its service to UV irradiation only. Thus, most of the solar irradiation ($\sim 95\%$) cannot be benefited by the TiO_2 photocatalyst. Metal ion doping into TiO_2 has been investigated for providing absorbance also in the visible region. Another aid of doping TiO_2 with metal ions in proper amounts, was suggested to be suppressing of the hole–electron recombination. Electron–hole recombination is detrimental for photocatalytic activity and it decreases efficiency of photocatalyst [9, 10].

Photocatalytic activity of TiO_2 , doped with metal ions such as Al^{3+} , V^{5+} , Cr^{3+} , Mn^{2+} , Fe^{3+} , Zn^{2+} , Sn^{4+} , and Ce^{4+} , has been investigated [5, 11–14]. Type and amount of doping is important in enhancing the photoactivity of TiO_2 under UV and visible light. Dopants, in specific ranges depending on the type of the dopant, were reported to be effective in augmenting the photocatalytic activity of TiO_2 . On the other hand, ratios of dopants out of the proper range were harmful [11, 13, 15, 16]. It is difficult to compare the activities or ratios of dopants in TiO_2 reported in different studies in literature, since TiO_2 was prepared by various methods and doping contents were reported in various forms like mole %, wt. %, or wt. % of dopant compound for instance in the form of metal nitrate, etc. [17].

Photoactivity of Sn doped TiO_2 powder has been investigated [12–15, 18], and 5% Sn was reported to enhance the activity of TiO_2 [12, 13]. The positive effects of SnO_2 and also of other dopants was proposed to be introducing new electronic states into the band gap of TiO_2 , decreasing the TiO_2 particle size and increasing the surface area thereby providing higher adsorption, and separation of the charge carriers [14, 15, 18].

TiO_2 powders, doped with different metal ions were prepared via various techniques such as sol–gel [11–14], hydrolysis of inorganic salts [19], ultrasonic technique [20] and hydrothermal method [13, 21–23]. The extent of doping depends on the type of the synthesis method. In most of the processes, a calcinations step is required in order to attain the crystal structure of TiO_2 . Calcination results in growth of TiO_2 grains, leading to loss of surface area and loss of photocatalytic efficiency [21]. Hydrothermal process is a relatively low temperature technique, in which the reaction takes place in a closed autoclave under high vapor pressure. Good control of the composition of the products is achieved in hydrothermal process and calcination of the products is mostly not necessary. It is environmentally friendly since reactions proceed in a closed system [21, 22, 24]. The need for an expensive

autoclave may be counted as the drawback of this process. Reflux synthesis is also a low temperature method. In this method the reaction takes place in a heated container, which is connected to a reflux condenser system open to atmosphere. The vaporized solvents are condensed back into the reaction medium and long lasting reactions can be accomplished.

Aim of this study is to prepare Sn doped TiO_2 nanoparticles by two different techniques, namely reflux and hydrothermal methods, and to investigate the photocatalytic activity of the formed powders. These methods were selected due to their low process temperature and lack of necessity for calcination of the products. For this purpose, photocatalytic degradation of malachite green (MG), a dye that is commonly used in textile industry, was tested in the presence of prepared TiO_2 powders by two different methods.

2 Materials and methods

2.1 Chemicals and apparatus

The reagents employed were titanium (IV)-*n*-butoxide [$\text{Ti}(\text{O}i\text{Bu})_4$, 97%, Fluka] as TiO_2 source, hydrochloric acid (Merck, 37%) as catalyst, tin (IV) chloride (Alfa Aesar, 98%) as dopant, deionized water as hydrolysis agent. Malachite Green (MG) was used as a model pollutant (analytical reagent grade).

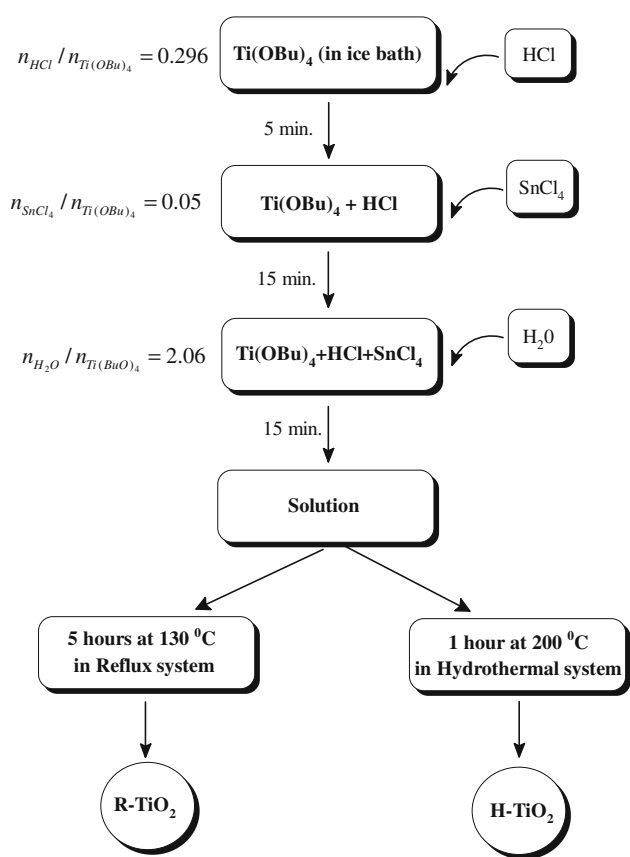
Nano- TiO_2 powders were synthesized by two different methods. In the first method, a Berghoff hydrothermal unit having time and temperature controllers was utilized. In the second method a condenser reflux system was used. A Rigaku Geigerflex D Max/B model X-ray diffractometer (XRD) with Cu $K\alpha$ radiation ($\lambda = 0.15418$ nm) in the region $2\theta = 10^\circ$ – 70° with a step size of 0.04° was used for determining the crystalline phases.

Size of Sn doped TiO_2 particles was investigated by transmission electron microscopy (TEM, FEI Tecnai G2F30). Elemental composition of the particles was investigated by flame atomic absorption spectroscopy (FAAS).

Dye concentration in the aqueous solution was measured in predetermined durations after irradiation by a Varian Carry 5000 model UV–vis–NIR spectrophotometer. Sn doped TiO_2 /dye solution was irradiated with/without 400 nm cut-off filter in a solar box (Erichsen, Model 1500) with an Xe lamp (690 W/m^2).

2.2 TiO_2 powder synthesis

Flowsheets for hydrothermal and reflux syntheses are presented in Scheme 1.



Scheme 1 Preparation steps and parameters of TiO₂ by hydrothermal and reflux methods

2.2.1 Hydrothermal method

Ti(OBu)ⁿ₄ was cooled in an ice-bath, then HCl (37% w/w) was added within 15 min into the cooled Ti(OBu)ⁿ₄ dropwise by a burette. After stirring for 5 min at ambient temperature, required amount of tin (IV) chloride was added. Final solution was stirred until a clear and homogeneous solution was formed. Then, required amount of water was added within 10 min into the solution dropwise by a burette. HCl/Ti(OBu)ⁿ₄, SnCl₄/Ti(OBu)ⁿ₄ and H₂O/Ti(OBu)ⁿ₄ mol/mol ratios were 0.296, 0.05 and 2.06, respectively. Gelation occurred after water addition. Reaction was allowed for 2 h, and then a viscose solution was obtained. The solution was transferred into a 250 mL Teflon bomb which was then closed. The closed bomb was placed inside a preheated (200 °C) stainless steel autoclave. Reaction was conducted at 200 °C for 1 h. The Teflon bomb was removed from the hydrothermal unit and it was cooled to room temperature. Obtained powders were separated by centrifuging and they were dried in a vacuum sterilizer. Thus, nanosized TiO₂ particles having yellow color were obtained.

2.2.2 Reflux method

Nano-TiO₂ particles were synthesized with the same molar ratios as mentioned above. The reaction was carried out in a glass balloon which was heated in an oil bath at 130 °C for 5 h. The balloon was connected to a reflux condenser system open to atmosphere.

2.3 Preparation of TiO₂ sols

TiO₂ (0.625 g) sols were prepared by ultrasonically dispersing the synthesized TiO₂ powder in deionized water (for H-SnTiO₂), and in water: n-propanol (for R-SnTiO₂) (1:1, w/w) mixture without using a dispersant. The solvents and TiO₂ particles were treated in an ultrasonic bath for a few minutes. Finally, transparent TiO₂ sols were obtained.

2.4 Photocatalytic degradation of malachite green

For photocatalytic decomposition experiments, 62.5 μL of dye solution (from 2.5 ppm stock solution of MG) was added into TiO₂ sol (24.94 mL, 2.5% TiO₂ (w/w)). The light of the empty solar box was kept on for 15 min for stabilization before starting the test. Meanwhile, the nano-TiO₂/MG sol was poured into the transparent polystyrene reaction cell consisting of 12 separate compartments. The cell was placed into the Solar Box. The decomposition of MG was monitored by measuring the absorbance at 617 nm (λ_{max}) by UV–VIS spectrophotometer. Decomposition of MG was quantified by detecting the MG concentration after 20, 40 and 60 min during UV and VIS—irradiation.

3 Result and discussions

3.1 Structure of TiO₂ powders

XRD patterns of Sn doped TiO₂ powders prepared by hydrothermal and reflux methods are presented in Fig. 1. It was seen that TiO₂ powders synthesized by both methods had anatase crystal structure. All the peaks of anatase phase TiO₂ could be clearly determined on the XRD patterns of the synthesized powders. Peaks of rutile and brookite phases, which are known to have less photocatalytic effect, were not present. The peaks on the XRD patterns at 25.39°, 38.11°, 48.47° and 55.01° pertaining to (101), (004), (200) and (211) planes matched well with those of anatase TiO₂ reported in literature [25] (ICDD card no: 21-1272). The peaks were seen to be wide, which can be taken as an indication of the nanometric size of the TiO₂ crystallites.

Particle size distributions of the synthesized TiO₂ powders which were determined by a Malvern Zetasizer Z/S unit are presented in Fig. 2. TiO₂ powder which was

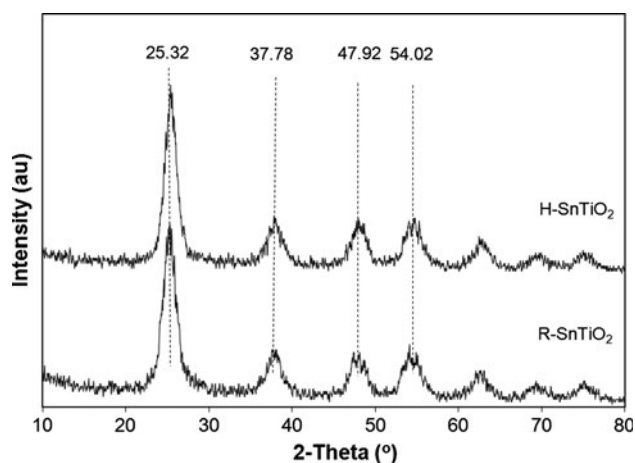


Fig. 1 XRD patterns of Sn doped TiO₂ powders synthesized by hydrothermal (H-SnTiO₂) and reflux (R-SnTiO₂) methods

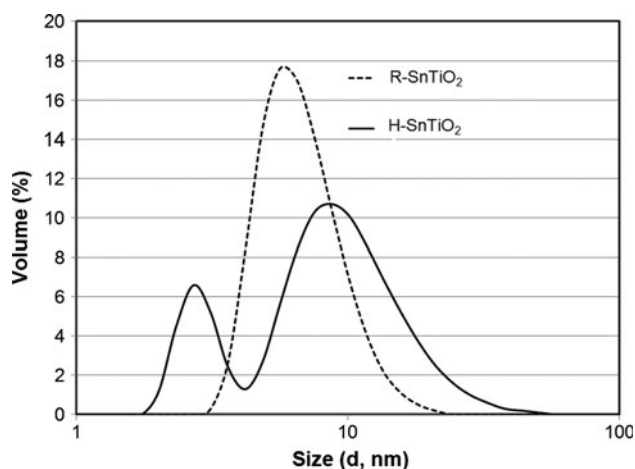


Fig. 2 Particle size distribution plots of Sn doped TiO₂ powders synthesized by hydrothermal (H-SnTiO₂) and reflux (R-SnTiO₂) methods

synthesized by reflux method had an average particle size of 7 nm. On the other hand, hydrothermally synthesized TiO₂ presented a bimodal particle size distribution with average particle sizes of about 3 and 10 nm. Formation of larger particles in hydrothermal synthesis as compared to reflux method may be due to higher temperature utilized in this process. Hydrothermal synthesis was conducted at 200 °C, whereas in reflux method temperature was kept at 130 °C. Surface areas of the Sn doped TiO₂ powders

synthesized by hydrothermal and reflux methods were 130 and 115 m²/g, respectively. Comparison of the particle size and specific surface area of TiO₂ powders is presented in Table 1. Photocatalytic activity of nano TiO₂ powder is strongly related to particle size and specific surface area. The lower is the particle size and the higher is the specific surface area, the higher is the photocatalytic effect. In the employed methods, crystalline anatase phase TiO₂ was obtained at low temperatures and as a result the calcination step was avoided. This helped preserving the nanostructure of the TiO₂ particles. Therefore, the obtained powders in both methods presented high specific surface areas.

TEM micrographs the TiO₂ powders which were obtained by hydrothermal and reflux methods are presented in Fig. 3a, b c, d respectively. In the presented TEM micrographs sizes of the individual particles can be visualized to be in nanometric scale. The particle sizes observed in the TEM micrographs are in accord with the particle sizes which were measured by Zetasizer Nano Z/S as presented in Fig. 2. TiO₂ particles are about 5 nm as shown in Fig. 3.

The molar ratio of Sn to Ti was kept at 5–95 as shown in Scheme 1. This amount of Sn corresponds to 4.71 mol % (or 6.83 wt%) in the total amount of synthesized Sn doped TiO₂ powders. The filtrate solutions after reflux synthesis and hydrothermal synthesis were analyzed by FAAS and it was determined that formed TiO₂ contained 5.9 wt% Sn and 6.54 wt% Sn, respectively. These results indicate that 86.38% of the Sn in reflux synthesis and 95.75% of Sn in hydrothermal synthesis were incorporated into the TiO₂ lattice structure. Higher doping amount of Sn into TiO₂ in hydrothermal synthesis may be due to higher temperature applied in this method and also may be due to high pressure provided in the autoclave.

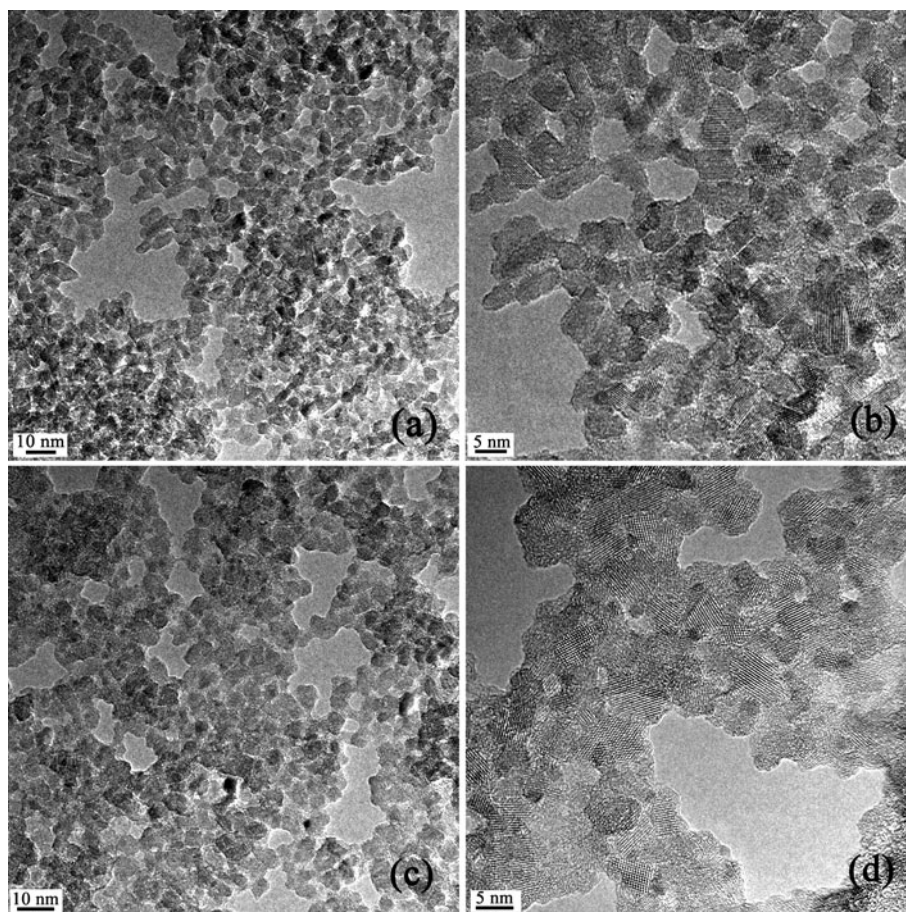
3.2 Photocatalytic activity tests

Photocatalytic effects of Sn doped TiO₂ powders obtained by the two methods were investigated by keeping 2.5 ppm MG in 2.5% (w/w) TiO₂ sol for 20–60 min under UV and VIS light in a solar box and by measuring the absorbance of MG by spectrophotometer. Height of the MG peak at 617 nm corresponds to the concentration of MG in solution. Height of the peak of MG was measured and thus % decomposition of MG as a result of photocatalytic reaction

Table 1 Properties and photocatalytic activities of synthesized powders

	Average particle size (nm)	Specific surface area of powder (m ² /g)	Sn doping achieved (%)	Degradation % of MG in visible light in 60 min.	Degradation % of MG in UV light in 60 min.
H-TiO ₂	3, 10	130	95.8	81	90
R-TiO ₂	7	115	86.4	61	92

Fig. 3 TEM micrographs of TiO_2 powder agglomerates formed in **a, b** hydrothermal synthesis and **c, d** reflux synthesis



was determined by following the decrease of the peak height. The results are presented in Fig. 4. Photocatalytic activity of hydrothermally synthesized TiO_2 was seen to be considerably higher than that of reflux synthesized TiO_2 . This was an expected result since Sn doping achieved in hydrothermally synthesized TiO_2 was higher than that in reflux synthesized TiO_2 , as shown in Table 1 and Fig. 4. Sn doping causes a shift in the absorbance of the TiO_2 powders into visible region [22]. Higher Sn dopant amount leads to larger absorbance, which results in higher photocatalytic activity under visible light. In addition, specific surface area of H-Sn TiO_2 was larger than that of R-Sn TiO_2 . This is another reason of higher photocatalytic activity of H-Sn TiO_2 . On the other hand in the UV illumination, photocatalytic activity of H-Sn TiO_2 was slightly higher than or similar to that of R-Sn TiO_2 as shown in Fig. 4. Slightly higher photocatalytic activity of H-Sn TiO_2 may be a consequence of its larger surface area.

It is difficult to compare the obtained results with those of the previous studies since in the literature decomposition of different organic agents at different concentrations was investigated. In the study of Liqiang et al. [26], Sn doped TiO_2 nano powder was obtained through sol-gel route by mixing $\text{Ti}(\text{O}i\text{Bu})_4$, ethanol, H_2O and HNO_3 . Products were calcined at

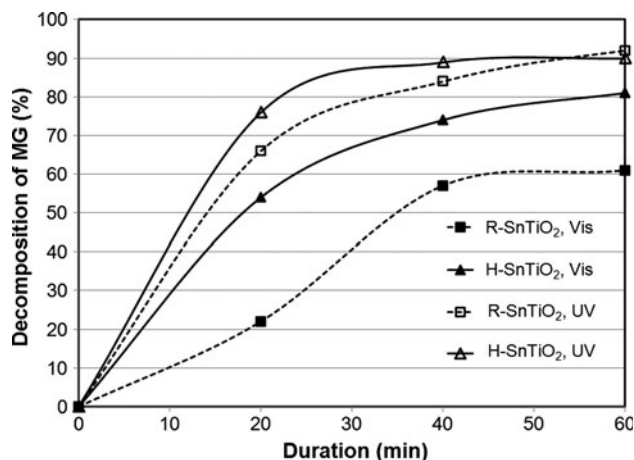


Fig. 4 Decomposition plots of MG via photocatalytic reaction of Sn doped TiO_2 powders synthesized by hydrothermal (H-Sn TiO_2) and reflux (R-Sn TiO_2) methods

500–700 °C. Photocatalytic degradation of phenol was the highest (20% degradation in 1 h) when the powder was calcined at 600 °C. In another study, Sn doped TiO_2 was utilized in the form of films on glass surfaces by Sayilkan et al. [27]. MG degradation of the obtained films were much lower when compared to that of the Sn doped TiO_2 powders in the present

study. In 1 h, degradation of MG was reported to be less than 50%. This is an expected result since the surface area of the film is lower than that of TiO₂ in powder form.

4 Conclusion

Synthesis of 5 mol % Sn doped TiO₂ (Sn to Ti molar ratio 5/95) nanopowders were accomplished through hydrothermal and reflux methods at 200 and 130 °C, respectively. Both methods produced anatase phase TiO₂ at low temperatures therefore calcination of obtained powders was not necessary. Hydrothermally synthesized TiO₂ powder presented higher photocatalytic activity than that of reflux synthesized TiO₂. This was attributed to higher Sn content as well as larger specific surface area of hydrothermal TiO₂. Reflux method is advantageous in terms of lower equipment cost and less labor over hydrothermal synthesis. Further adjustment of experimental parameters of reflux synthesis such as lower temperature and longer duration may result in formation of TiO₂ powders having higher Sn content and higher specific surface area. Hazardous effects of organic contaminants to the environment can be prevented by the use of photocatalytic TiO₂ powder prepared by hydrothermal or reflux synthesis.

Acknowledgments Authors would like to thank Akdeniz University Research Fund for financial support. Technical and financial support of T.R. Prime Ministry State Planning Organization (Project number: 2005 DPT.120.150) and NANOen are gratefully acknowledged.

References

- Chen X, Mao SS (2007) Titanium dioxide nanomaterials: synthesis, properties, modifications, and applications. *Chem Rev* 107:2891–2959
- Fujishima A, Zhang X, Tryk DA (2008) TiO₂ photocatalysis and relate surface phenomena. *Surf Sci Rep* 63:515–582
- Lasa H, Serrano B, Salaces M (2005) Photocatalytic reaction engineering. Springer Science+Business Media Inc, New York
- Kesmez Ö, Çamurlu HE, Burunkaya E, Arpaç E (2009) Sol–gel preparation and characterization of anti-reflective and self-cleaning SiO₂–TiO₂ double-layer nanometric films. *Sol Energy Mater Sol Cells* 93:1833–1839
- Burunkaya E, Kesmez Ö, Kiraz N, Çamurlu HE, Asiltürk M, Arpaç E (2010) Sn⁴⁺ or Ce³⁺ doped TiO₂ photocatalytic nanometric films on antireflective nano-SiO₂ coated glass. *Mater Chem Phys* 120:272–276
- Liu Z, Zhang X, Murakami T, Fujishima A (2008) Sol-gel SiO₂/TiO₂ bilayer films with self-cleaning and antireflection properties. *Sol Energy Mater Sol Cells* 92:1434–1438
- Wu T, Liu G, Zhao J, Hidaka H, Serpone N (1998) Photoassisted degradation of dye pollutants. V. self-photosensitized oxidative transformation of rhodamine B under visible light irradiation in aqueous TiO₂ dispersions. *J Phys Chem B* 102:5845–5851
- Asiltürk M, Sayılkan F, Erdemoğlu S, Akarsu M, Sayılkan H, Erdemoğlu M, Arpaç E (2006) Characterization of the hydrothermally synthesized nano-TiO₂ crystallite and the photocatalytic degradation of Rhodamine B. *J Hazard Mater B* 129:164–170
- Bellardita M, Addamo M, Di Paola A, Palmisano L (2007) Photocatalytic behaviour of metal-loaded TiO₂ aqueous dispersions and films. *Chem Phys* 339:94–103
- Shi JW, Zheng JT, Wu P (2009) Preparation, characterization and photocatalytic activities of holmium-doped titanium dioxide nanoparticles. *J Hazard Mater* 161:416–422
- Yao M, Chen J, Zhao C, Chen Y (2009) Photocatalytic activities of Ion doped TiO₂ thin films when prepared on different substrates. *Thin Solid Films* 517:5994–5999
- Liu B, Zhao X, Zhang N, Zhao Q, He X, Feng J (2005) Photocatalytic mechanism of TiO₂–CeO₂ films prepared by magnetron sputtering under UV and visible light. *Surf Sci* 595:203–211
- Sayılkan F, Asiltürk M, Tatar P, Kiraz N, Arpaç E, Sayılkan H (2007) Photocatalytic performance of Sn-doped TiO₂ nanostructured mono and double layer thin films for Malachite Green dye degradation under UV and vis-lights. *J Hazard Mater* 144:140–146
- Caimei F, Peng X, Yanping S (2006) Preparation of Nano-TiO₂ doped with cerium and its photocatalytic activity. *J Rare Earth* 24:309–313
- Stengl V, Bakardjieva S, Murafa N (2009) Preparation and photocatalytic activity of rare earth doped TiO₂ nanoparticles. *Mater Chem Phys* 114:217–226
- Wang Z, Chen C, Wu F, Zou B, Zhao M, Wang J, Feng C (2009) Photodegradation of rhodamine B under visible light by bimetal codoped TiO₂ nanocrystals. *J Hazard Mater* 164:615–620
- Di Paola A, Garcia-Lopes E, Ikeda S, Marci G, Ohtani B, Palmisano L (2002) Photocatalytic degradation of organic compounds in aqueous systems by transition metal doped polycrystalline TiO₂. *Catal Today* 75:87–93
- Chen X, Mao SS (2007) Titanium dioxide nanomaterials: synthesis, properties, modifications, and applications. *Chem Rev* 107:2891–2959
- Zhang Y, Xiong G, Yao N, Yang W, Fu X (2001) Preparation of titania-based catalysts for formaldehyde photocatalytic oxidation from TiCl₄ by the sol–gel method. *Catal Today* 68:89–95
- Wu XM, Wang L, Tan ZC, Li GH, Qu SS (2001) Preparation, characterization and low-temperature heat capacities of nanocrystalline TiO₂ ultrafine powder. *J Solid State Chem* 156:220–224
- Akarsu M, Asiltürk M, Sayılkan F, Kiraz N, Arpaç E, Sayılkan H (2006) A novel approach to the hydrothermal synthesis of anatase Titania nanoparticles and the photocatalytic degradation of rhodamine B. *Turk J Chem* 30:333–343
- Arpaç E, Sayılkan F, Asiltürk M, Tatar P, Kiraz N, Sayılkan H (2007) Photocatalytic performance of Sn-doped and undoped TiO₂ nanostructured thin films under UV and vis-lights. *J Hazard Mater* 140:69–74
- Vigil E, Ayllon JA, Peiro AM, Clemente RR (2001) TiO₂ layers grown from flowing precursor solutions using microwave heating. *Langmuir* 17:891–896
- Burunkaya E, Kiraz N, Kesmez Ö, Çamurlu HE, Asiltürk M, Arpaç E (2010) Preparation of aluminum-doped zinc oxide (AZO) nano particles by hydrothermal synthesis. *J Sol-Gel Sci Technol* 55:171–176
- Kartini I, Meredith P, Diniz Da Costa JC, Lu GQ (2004) A novel route to the synthesis of mesoporous Titania with full anatase nanocrystalline domains. *J Sol-Gel Sci Technol* 31:185–189
- Liqiang J, Honggang F, Baiqi W, Dejun W, Baifu X, Shudan L, Jiazhong S (2006) Effects of Sn dopant on the photoinduced charge property and photocatalytic activity of TiO₂ nanoparticles. *Appl Catal B Environ* 62:282–291
- Sayılkan F, Asiltürk M, Tatar P, Kiraz N, Şener Ş, Arpaç A, Sayılkan H (2008) Photocatalytic performance of Sn-doped TiO₂ nanostructured thin films for photocatalytic degradation of malachite green dye under UV and VIS-lights. *Mater Res Bull* 43:127–134